Multilayers at Interfaces of an Oppositely Charged Polyelectrolyte/Surfactant System resulting from the Transport of Bulk Aggregates under Gravity

Richard A. Campbell[1], Marianna Yanez Arteta[2],*

Anna Angus-Smyth[1,3], Tommy Nylander[2] and Imre Varga[4]*

1. Institut Laue-Langevin, 6 rue Jules Horowitz, BP 156, 38042 Grenoble Cedex 9, France

2. Department of Physical Chemistry, Lund University, P. O. Box 124, S-221 00 Lund, Sweden

3. Department of Chemistry, Durham University, South Road, DH1 3LE, United Kingdom

4. Institute of Chemistry, Eötvös Loránd University, Budapest 112, P. O. Box 32, H-1518 Hungary

Electronic Supporting Information: Density Calculations & Multilayer Simulations

1. Density Calculations.

We know from small-angle X-ray and neutron scattering measurements that Pdadmac/SDS aggregates in the bulk have structures with a hexagonal phase, i.e., elongated surfactant micelles with the headgroups interacting with solvated polymer chains in a 2D hexagonal arrangement.[ESI1,ESI2] Based on this structure and some simple assumptions regarding the internal organization of the complex, as described schematically in Figure ESI1, we can estimate the composition of the aggregates following an approach similar to that in ref. ESI3. Ideal swelling of the hexagonal phase can be expressed as

$$\phi_P + \frac{2\pi R^2}{\sqrt{3}\,a^2} = 1 \qquad \text{(ESI1)}$$

with R the radius of the alkyl chain region of the surfactant cylinders, a the lattice spacing which can be calculated from the d-spacing by $a = 2d/\sqrt{3}$, and ϕ_P the polar volume fraction.

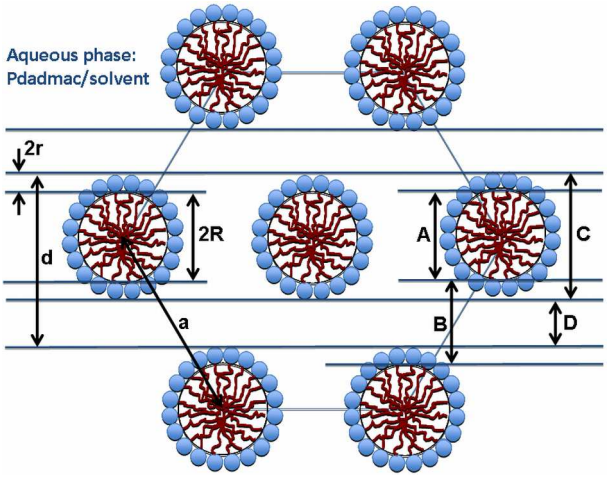

Figure ESI1. Schematic representation of the Pdadmac/SDS hexagonal phase aggregates.

The Bragg diffraction peak measured for the Pdadmac/SDS aggregates corresponds to a d-spacing of 36.0 ± 0.5 Å, which gives a = 41.6 Å. We assume that the cylinders are much longer than their diameter and take the surfactant chain radius of each cylindrical micelle from that corresponding to wormlike micelles of SDS in NaBr as R = 12 Å.[ESI4] If we insert the known values in the expression for ϕ_P in eq. ESI1, the volume fraction of the non-polar part, $1 - \phi_P = 0.302$. The volume fraction of the polar part can be expressed as $\phi_P = \phi_{SDS\text{-}head} + \phi_{Pdadmac} + \phi_{solv,}$ which are terms for the volume fractions of the surfactant headgroups, polymer and solvent, respectively. The volume of a single dodecyl chain may be calculated as 352 Å^3,[ESI5] and the volume of the sulfate headgroup may be taken as 51 Å^3.[ESI6] As each surfactant headgroup is chemically bonded to one dodecyl chain, the volume fraction of the surfactant headgroup, $\phi_{SDS\text{-}head} = (51/352) \times (1 - \phi_P) = 0.044$. To estimate the volume fraction of polymer, we take the simplest approach and assume a stoichiometric amount of Pdadmac and SDS in the absence of the counterions. This approach may be justified by the fact that the phase separation region comprises aggregates close to charge neutrality of the bulk complexes. The volume of Pdadmac monomers may be taken as 137 cm^3/mol,[ESI7] i.e., 228 Å^3 per monomer. Here we need to correct for the absent counterion by subtracting the volume of a chloride ion, which may be taken as 25 Å^3,[ESI6] giving a total volume of 203 Å^3 per monomer. Thus $\phi_{Pdadmac} = (203/352) \times (1 - \phi_P) = 0.174$. The volume fraction of the solvent may then be calculated by $\phi_{solv} = \phi_P - \phi_{SDS\text{-}head} - \phi_{Pdadmac} = 0.480$. Table ESI1 lists the calculated relative volumes of the components in hexagonal phase neutral Pdadmac/SDS aggregates.

Our calculations form the basis of the multilayer simulations below, so they must be consistent with our UV-vis spectroscopy data shown in fig. 3 of the main text. To validate the parameters derived for the multilayer simulations, therefore, we can demonstrate that we can take the aggregate structure and calculate the relative densities between the aggregates and solvent for each isotopic contrast to correlate qualitatively the trends in the measured relative creaming or sedimentation rates.

Table ESI1. Volume fractions of components in hexagonal Pdadmac/SDS aggregates.

Species	Volume fraction
Surfactant chains	0.302
Surfactant headgroups	0.044
Polymer segments	0.174
Solvent	0.480

The density of Pdadmac is 1.179 g/cm^3 calculated from the product information. Again, the correction for the absent counterion (chloride this time) must be carried out to give a monomer volume of 203 Å^3 = 122.2 cm^3/mol, a molar mass of 126.2 g/mol and a revised density of 1.033 g/cm^3. The same approach may be used for the surfactant, using the volume of 4 Å^3 for the sodium ion.[ESI6] For hSDS we have a molecular volume of 352 Å^3 for the chain and 51 Å^3 for the headgroup from above, so with a molar mass of 265.4 g/mol (in the absence of the counterion) the density is 1.094 g/cm^3. The corresponding value for dSDS is 1.196 g/cm^3. The bulk liquid densities at 25 °C are 0.997 g/cm^3 for H_2O,[ESI8] and 1.105 g/cm^3 for D_2O[ESI9] which can be corrected for isotopic exchange to 1.099 g/cm^3 according to the fitted scattering length density of the solvent in ref. ESI10. From the individual volume fractions listed in table ESI1, we can now derive the relative densities of the aggregates and solvent in the three isotopic contrasts studied, which are listed in table ESI2.

Table ESI2. Relative densities of Pdadmac/SDS aggregates and solvent.

Isotopic contrast	Aggregate density, ρ_{agg} (g/cm^3)	Solvent density, ρ_{sol} (g/cm^3)	Density difference, $\Delta\rho = \rho_{agg} - \rho_{sol}$ (g/cm^3)
Pdadmac/hSDS/D_2O	1.086	1.099	–0.013 upward
Pdadmac/hSDS/H_2O	1.037	0.997	0.040 downward
Pdadmac/dSDS/ACMW	1.076	1.006	0.070 downward
Pdadmac/dSDS/H_2O	1.072	0.997	0.075 downward

The density differences between the bulk aggregates and solvent are qualitatively consistent with the UV-vis spectroscopy data of the creaming and sedimentation of Pdadmac/SDS aggregates shown in fig. 3 of the main text, i.e., Pdadmac/dSDS/H_2O > Pdadmac/hSDS/H_2O > Pdadmac/hSDS/D_2O. Further, they show a ratio of 5:1 for Pdadmac/dSDS/ACMW (down) to Pdadmac/hSDS/D_2O (up) relevant to the air/liquid measurements in figs. 4 and 5 of the main text, and a ratio of 6:1 for Pdadmac/dSDS/H_2O (down) to Pdadmac/hSDS/D_2O (up) relevant to the solid/liquid measurements in fig. 6 of the main text. These calculations also help us to rationalize the negligible surface structure in the Pdadmac/dSDS/H_2O

contrast for air-above-liquid and solid-above-liquid (sample 3) measurements as well as in the Pdadmac/hSDS/D_2O contrast for solid-below-liquid (sample 2) measurements. Also, they are qualitatively consistent with a larger ratio of the Bragg peak area for Pdadmac/dSDS/H_2O solid-below-liquid (sample 4) to Pdadmac/hSDS/D_2O solid-above-liquid (sample 1) than that derived from the multilayer simulations of the same chemical interfaces in fig. 7 of the main text.

2. Multilayer Simulations.

For these simulations, we model the contrasts Pdadmac/hSDS/D_2O and Pdadmac/dSDS/H_2O in the solid/liquid experiment (fig. 7 in the main text), and Pdadmac/hSDS/D_2O and Pdadmac/dSDS/ACMW (91.9% H_2O in D_2O) in the air/liquid experiments (fig. 8 in the main text). Again, we note that the latter solvent of ACMW was used instead of H_2O due to practical reasons as the original intention of recording the data was to determine the interfacial composition of the molecular adsorption layer, but the salient point for the present work is that the density of ACMW is very close to that of H_2O (< 1 % difference). Table ESI3 gives the scattering length densities of the individual components.

Table ESI3. Relative volumes and scattering length densities of components in the hexagonal Pdadmac/SDS aggregates.

Species	Molecular/Monomer Volumes ($Å^3$)	Scattering length density (x 10^{-6} $Å^{-2}$)
dSDS chains	352	7.00
hSDS chains	352	–0.39
Sulfate headgroups	51	5.11
Polymer segments	203	0.13
D_2O	30	6.31*
H_2O	30	–0.56
ACMW	30	0.00

* Note that this value was derived from fitting the critical edge of air/D_2O NR data in ref. ESI10.

The simulations were carried out by approximating the surface structure to a stratified layer model where the d-spacing of the Bragg peak equals the repeat distance d in fig. ESI1. As input parameters for the multilayer simulations we divide the structure into two slabs, one surfactant-rich (A) and one polymer-rich (B), as shown schematically in fig. ESI1. In this case the boundaries between slabs were positioned at the outside of the hydrophobic core of the micelles. The thickness of each slab is 2R = 24.0 Å for slab A (containing the surfactant alkyl chains), and d – 2R = 12.0 Å for slab B (polar). By approximating each surfactant micelle into an inner circular region for the chains and an outer circular

region for the headgroups the fraction of headgroups in slab A may be calculated geometrically as 0.649. The volume fraction of the headgroups from table ESI1 may therefore be split accordingly into the two slabs and normalized to the relative layer thicknesses. All of the surfactant chains are located in slab A so the corresponding volume fraction from table ESI1 simply needs to be normalized according to the relative layer thicknesses. In both slabs the remaining volume fraction (0.504 for slab A and 0.954 for slab B) may be filled with polyelectrolyte and solvent in the proportion indicated by the overall volume fractions in table ESI1. The volume fractions of components in each slab are listed in table ESI4.

Table ESI4. Volume fractions of species in hexagonal Pdadmac/SDS aggregates.

Species	Volume fraction of slab A* with thickness 24.0 Å	Volume fraction of slab B* with thickness 12.0 Å
Surfactant chains	0.453	0.000
Surfactant headgroups	0.043	0.046
Polymer segments	0.134	0.254
Solvent	0.370	0.700

* Slab A contains the surfactant alkyl chains while slab B is polar according to boundaries shown in fig. ESI1

Table ESI5 lists the scattering length densities of the appropriate slabs in the three measured isotopic contrasts; note that the mixing length scales within the aqueous region are well below the coherence length of the neutrons and therefore may simply be averaged.

Table ESI5. Scattering length densities and layer thickness for the slabs used in the multilayer simulations of hexagonal phase Pdadmac/SDS aggregates.

Isotopic contrast	Scattering length density ($\times 10^{-6}$ Å^{-2}) of slab A* with thickness 24.0 Å	Scattering length density ($\times 10^{-6}$ Å^{-2}) of slab B* with thickness 12.0 Å
Pdadmac/hSDS/D_2O	2.40	4.69
Pdadmac/dSDS/ACMW	3.41	0.27
Pdadmac/dSDS/H_2O	3.20	–0.12

* Slab A contains the surfactant alkyl chains while slab B is polar according to boundaries shown in fig. ESI1

Multilayer simulations in figs. 7 and 8 of the main text were carried out using Motofit software[ESI11] using the parameters derived in table ESI5 and fitted values for the measured background. The aim was to examine the relative areas of a Bragg peak from the surface structure of chemically identical samples with different isotopic contrasts at the solid/liquid interface for Pdadmac/hSDS/D_2O + interface-above-

liquid (sample 1) and Pdadmac/dSDS/H_2O + interface-below-liquid (sample 4) in fig. 6 of the main text and at the air/liquid interface in fig. 4 of the main text, respectively. In the latter case the same molecular layer structure was used as that in our recent paper about Pdadmac/SDS layers at the air/liquid interface, i.e., a surfactant monolayer with a solvated polyelectrolyte layer attached electrostatically to the headgroups.[ESI10] An equivalent layer structure was used at the hydrophobic solid/liquid interface in the former case allowing for reasonable estimations of the silicon dioxide and silane layers.

The interplay between the number of repeating units (chosen arbitrarily to be 100) and the coverage of the multilayer aggregates (7.8 % for the air/liquid data and 10.2 % for the solid/liquid data), and details concerning the underlying properties of the fixed and molecular adsorption layers, both had minimal effects on the derived ratios, which were principally determined by the relative scattering contrasts of the different regions within the aggregates. Furthermore, tests of the robustness of the model showed that changing the choice of boundaries from the outside of the hydrophobic core of the micelles with slabs A and B to the outside of the hydrophilic headgroups with slabs C and D (see fig. ESI1) resulted in a change in the derived ratios of just 8 % for the air/liquid experiment and 15 % for the solid/liquid experiment. Therefore we are satisfied that the choice of location of the slab boundaries in the applied model did not affect any of our interpretations or conclusions.

The output of the multilayer simulations as described in the Discussion section has allowed us to rationalize the relative Bragg peak areas in the different experiments with respect to the direction and rate of the mean transport of the bulk aggregates toward a given horizontal interface.

References

ESI1. Yeh, F.; Sokolov, E. L.; Walter, T.; Chu, B. *Langmuir* **1998**, *14*, 4350–4358.

ESI2. Sokolov, E. L.; Yeh, F.; Khokholov, A.; Grinberg, V. Y.; Chu, B. *J. Phys. Chem. B* **1998**, *102*, 7091–7098.

ESI3. Ramos, L.; Ligoure, C. *Langmuir* **2008**, *24*, 5221–5224.

ESI4. Arleth, L.; Bergström, M.; Pedersen, J. S. *Langmuir* **2002**, *18*, 5343–5353.

ESI5. Vass, S.; Török, T.; Jákli, G.; Berecz, E. *J. Phys. Chem.* **1989**, *93*, 6553–6559.

ESI6. Marcus, Y. “Ion Properties”, Marcel and Dekker, New York, 1997.

ESI7. Wandrey, C.; Bartkowiak, A.; Hunkeler, D. *Langmuir* **1999**, *15*, 4062–4068.

ESI8. Kell, G. S. Density, Thermal Expansivity, and Compressibility of Liquid Water from 0 to 150 °C, Journal of Chemical and Engineering Data, 1975, Vol.20, No.1, pp.97–105 (Equation 16).

ESI9. Handbook of Chemistry and Physics, 73rd Edition, Lide, D.R. Ed.; CRC Press: Boca Raton 1992; Chapter 6, p. 13.

ESI10. Campbell, R. A.; Arteta, M. Y.; Angus-Smyth, A.; Nylander, T.; Varga, I. *J. Phys. Chem. B* **2011**, *115*, 15202–15213.

ESI11. Nelson, A. *J. Appl. Crystallogr.* **2006**, *39*, 273–276.